Research Article

Cristiano Devitte*, Gabriel S. C. Souza, André J. Souza, and Volnei Tita

Optimization for drilling process of metal-composite aeronautical structures

https://doi.org/10.1515/secm-2021-0027
received November 26, 2020; accepted January 27, 2021

Abstract: Metal-composite laminates and joints are applied in aircraft manufacturing and maintenance (repairing) using aluminum alloys (AA) and glass fiber-reinforced polymer (GFRP). In these applications, drilling has a prominent place due to its vast application in aeronautical structures' mechanical joints. Thus, this study presents the influence of uncoated carbide drills (85C, 86C, H10N), cutting speeds (v_c = 20, 40, and 60 m min^{-1}), and feed rates (f = 0.05, 0.15, and 0.25 mm rev^{-1}) on delamination factor, thrust force (F_t), and burr formation in dry drilling metal-composite laminates and joints (AA2024/GFRP/AA2024). Experiments were performed, analyzed, and optimized using the Box–Behnken statistical design. Microscopic digital images for delamination evaluation, piezoelectric dynamometer for thrust force acquisition, and burr analysis were considered. The major finding was that the thrust force during drilling depends significantly on the feed rate. Another significant factor was the influence of the drill type (combined or not with feed rate). In fact, it was verified that the feed rate and the drill type were the most significant parameters on the delamination factor, while the feed rate was the most relevant on thrust force. The cutting speed did not affect significantly thrust force and delamination factor at exit (F_{da_S}). However, the combination $f \times v_c$ was significant in delamination factor at entrance (F_{da_E}). Based on the optimized input parameters, they presented lower values for delamination factors (F_{da_E} = 1.18 and F_{da_S} = 1.33) and thrust force (F_t = 67.3 N). These values were obtained by drilling the metal-composite laminates with 85C-tool, 0.05 mm rev^{-1} feed rate, and 20 m min^{-1} cutting speed. However, the burrs at the hole output of AA2024 were considered unsatisfactory for this specific condition, which implies additional investigation.

Keywords: drilling, metal-composite laminates, delamination factor, thrust force, Box–Behnken design

1 Introduction

The advent of new processing techniques and cutting tools ensures that composite and hybrid materials have been used in several engineering fields, especially in aeronautical, aerospace, and automobile industries [1,2]. Fiber-reinforced polymer matrix composites (FRPs) are widely used in the aerospace industry [1–6], with carbon (CFRP) and glass (GFRP) fibers being the most used reinforcements and, consequently, the most studied [3,6–8]. As it is known, in general, the mechanical properties of CFRP are superior to those of GFRP. However, the machinability of both materials is similar [9].

Manufacturers need to drill approximately one million holes in structural components to assemble one aircraft's fuselage in the aeronautical industry. In general, aeronautical structures consist of sheets made from different materials (such as sandwich panels) that are connected by mechanical joints (using fasteners) of metal/metal, metal/composite, and composite/composite parts [10]. The aerospace industry reaches 40 million holes per year, 80% of which are obtained manually, preceding mechanical fasteners [11]. About 60% of the hybrid structural components that are rejected by the aeronautical industry have defects directly related to the drilling process [6]. Combined with the parts' high added value, this fact makes drilling composite materials and metal-composite laminate subject to constant investigations [12].

The drilling of hybrid metal/composite stack is the main challenge due to different phenomena, such as delamination [5] and damage in the polymer matrix and fibers due to thermal gradients from metal chips [6]. Furthermore, it is challenging to select optimal cutting parameters and

* **Corresponding author: Cristiano Devitte,** Mechanical Engineering Department (DEMEC), Federal University of Rio Grande do Sul (UFRGS), 90050-170 Porto Alegre, RS, Brazil, e-mail: cristiano.devitte1@gmail.com, tel: +55-54-98427-8821
Gabriel S. C. Souza, Volnei Tita: Aeronautical Engineering Department, Sao Carlos School of Engineering, University of Sao Paulo (USP), 13563-120 Sao Carlos, SP, Brazil
André J. Souza: Mechanical Engineering Department (DEMEC), Federal University of Rio Grande do Sul (UFRGS), 90050-170 Porto Alegre, RS, Brazil

tools to guarantee machining quality and surface integrity for all constituents (fibers and matrix) [4,5].

Zitoune et al. [6,13] verified that the most common problems in drilling metal-composite laminate CFRP/Al were (i) damage due to the interaction between composite surface and continuous chips, which comes from machining Al; (ii) separation of composite ply from the metal ply due to high thrust forces, producing an accumulation of aluminum chips and fiber fragments at the CFRP/Al interface; and (iii) adhesion of a metallic layer along the entire cutting edge.

The CFRP delamination directly affects the quality of the assembly of hybrid structures. The degree of defects represents the drilling quality characterized by the so-called spalling at the hole exit. The feed rate effect is often higher than the spindle speed; then, it is necessary to control the thrust force when the chisel edge is in contact with the exit surface of the plate [14]. The mechanical performance of the metal-composite laminate stack decreases, especially when subjected to cyclic loads (fatigue), and can be mainly identified in the region of entry and exit of the cutting tool [1]. Damage caused by delamination in the tool exit is higher than that caused in the entrance [15,16]. The delamination in the tool entrance (peel-up) can be considered a consequence of the contact between the drill tip and upper layers of laminate. Conversely, in the tool exit (push-out), damage is caused by the compressive loadings applied by the end of the drill on the upper layers of the laminate [17]. The usage of the digital analysis is suitable to estimate damages after drilling. This kind of failure can be quantified using the delamination factor (F_d) that can be calculated through the ratio between the maximum diameter of the damaged area (D_{max}) and the tool diameter (D_o) as shown in equation (1) [18,19], considering the contribution of cracks in the area damaged by the process drilling holes. An adjusted delamination factor (F_{da}) was proposed by ref.[18], as shown in equation (2), which considers the influence of the damaged area (A_d). Besides, it used A_{max}, which is the area of the circumference calculated through D_{max}, and A_o is the area of the nominal circumference calculated using the drill diameter (D_o).

$$F_d = \frac{D_{max}}{D_o}. \tag{1}$$

$$F_{da} = F_d + \left(\frac{A_d}{A_{max} - A_o}\right)(F_d{}^2 - F_d). \tag{2}$$

Different authors concluded that the feed rate is the most relevant input parameter on delamination factor [16,21–28] and thrust force [20–22,24,26–29] during the drilling GFRP. Others have also verified the influence of the drill. Srinivasan et al. [25] showed that the drill diameter strongly influences the delamination results. Gaitonde et al. [27] showed that a lower point angle combined with the feed rate could reduce the damage. Batista et al. [26] confirmed that the tool geometry affects delamination and thrust force. Rubio et al. [29] also observed that the drill geometry and drill wear influence delamination and thrust force. Davim and Reis [30] identified that carbide is a better choice than HSS for drilling CFRP and null wear in the flank surface, while the HSS drill presents wear of 0.012 mm. Abrão et al. [31] verified the highest thrust force values for drills with three cutting edges. Rubio et al. [32] identified high-speed machining (HSM) contribution for drilling GFRP to ensure low damage levels.

Considering the process of generating through-holes in ductile metals by the drilling process with a twist drill, burrs may occur at the holes' exit. Furthermore, drills with smaller point angles generate higher forces and plastic deformation in the holes' central part, generating crown burrs. However, larger point angles can distribute better the forces at the periphery of the holes, causing a complete or partial fracture and generating smooth burrs, which are more easily removed. If a partial fracture takes place, a hat burr occurs [33]. Moreover, Pinto [34] found that drills with smaller helix angles generate the best results when thin sheets of AA2024 are drilled, mainly at the holes' exit, decreasing the subsequent deburring steps.

The deburring step, which is often required after the manufacturing process, is not usually done in an automated way but manual. Thus, it implies the qualified workforce, specific equipment, and process time increment, causing increased production costs [35–37].

Considering the scenario pointed earlier, the present work's contribution consists of finding the optimal combination for values of different parameters involved in the drilling process, such as the drill type, the cutting speed, and the feed rate to minimize the delamination factor, the thrust force, and burr formation generated during drilling of a hybrid composite laminate, AA2024/GFRP/AA2024 stack, applied in aeronautical structures. Thus, the Box–Behnken design (BBD) was performed for experimental analysis and input parameters optimization. Finally, based on the results, some relevant conclusions and recommendations are highlighted for the drilling of hybrid composite laminate joined by fasteners and used in aeronautical structures.

Table 1: Chemical composition of aluminum alloy AA2024 (wt%)

	Si	Fe	Cu	Mn	Mg	Cr	Zn	Ti	Al
Measured	0.07	0.2	3.5	0.3	1.3	0.01	0.1	0.03	Remainder
ASTM B209	<0.5	<0.5	3.8–4.9	0.3–0.9	1.2–1.8	<0.1	<0.25	<0.15	Remainder

2 Materials and methods

2.1 Hybrid composite stack

The metal-composite laminate used in the tests was obtained by stacking two AA2024 (Al) plates with 1.0 mm thickness and one plate of glass fiber-reinforced polymer (GFRP) with 5.0 mm thickness, forming a sandwich Al/GFRP/Al. Table 1 presents the chemical composition of AA2024 obtained through optical emission spectrometer brand Bruker model Q2ION and standardized by ASTM B209. The GFRP plate is made of glass fibers (reinforcement) and epoxy resin (matrix). In general, fibers used for lamination are found as blankets or fabrics [38]. In this study, the reinforcements are composed of type-E fiberglass fabric. The GFRP plate used 20 unidirectional layers of glass fibers, producing a composite plate with a 50% volume fraction of fibers.

2.2 Cutting tools

Sandvik® uncoated-carbide drills with 6.0 mm diameter and cross edging were used. These are recommended for drilling CFRP, GFRP, and stacking of plates with aluminum and titanium. Table 2 presents the drill tools specifications. The drill was mounted on a 6 mm diameter collet holder in a BT-30 morse taper (DIN 6499), both manufactured by Sandvik®. The run-out (δ) was verified for each tool assembly change with a Digimess dial gauge (resolution of 0.01 mm).

2.3 Experimental procedure

The experiment was carried out in a three-axis vertical machining center Romi® Discovery 308 (maximum power of 5.5 kW and maximum rotation of 4,000 rpm).

The input parameters were analyzed using three levels and combined according to the BBD, which is a method of statistical optimization that aims to change variables at three levels (−1, 0, +1) to develop a response surface. The design of experiments (DOE) consists of a combination of factor analysis and incomplete block designs [39] to reach the best levels according to the factors that influence a specific process. When three-factor, three-level BBD is used, 12 runs are required with combinations of the proposed variables, including three replicates at the center point (level 0), i.e., 15 runs. These replicates estimate the experimental variance and check the loss of linearity between the levels chosen for each variable. BBD also allows for optimization. It is

Table 2: Sandvik® drill tools specifications

Series	Precorp		CoroDrill 860
Type	85C	86C	H10N
			
σ (point angle) (°)	118	135	130
Chisel edge (µm)	73	93	120
φ (helix angle) (°)	27.6	26.6	16.6
Core thickness (mm)	1.45	2.11	1.85
R_a (average roughness) (µm)	0.10	0.15	0.17

Table 3: Three levels of input parameters

Control factors	Level		
	(−1)	(0)	(+1)
v_c (m min^{-1})	20	40	60
f (mm rev^{-1})	0.05	0.15	0.25
Drill type	86C	85C	H10N

based on the statistical analysis of the parameter's influence and the nature of the result [40]. Table 3 presents the parameters used and their levels.

The experimental design is presented in Table 4. From the definition of three control variables (input parameters), it is possible to identify four response variables (output parameters): (i) adjusted delamination factor at the tool entrance of the GFRP plate (F_{da_E}), (ii) adjusted delamination factor at the tool exit of the GFRP plate (F_{da_S}); (iii) thrust force in the cutting operation (F_t); and (iv) burr type generated at the tool exit of the AA2024 plate (Burr).

The thrust force (F_t) were measured by a Monitor System, which is composed of a Kistler® 9272 stationary piezoelectric dynamometer four-component, a Kistler® 5070A charge amplifier, a DAQ board, and a dedicated PC with LabVIEW™ 9.0. The acquisition rate was 1.0 kS/s. Sixteen holes were made in the metal-composite laminate for fixing (Figure 1a) the plate as shown in Figure 1b.

Pretests (preliminary tests) were also carried out. The positions of the holes have been optimized for maximum usage of the plates, where the minimum distance between centers was equal to $2.5\,D$ to measure the F_t over the 314 cm^2 circular area of the dynamometer surface.

The hole images in detail were obtained using a digital microscope Dino-Lite AM-413ZT with 30x magnification after the experiment (Figure 2a). The Image-J

Table 4: Response variables and control factors

Run order	Control factors			δ (mm)	Response variables			
	v_c (m min^{-1})	f (mm rev^{-1})	Drill type		F_{da_E}	F_{da_S}	F_t [N]	Burr*
1	60	0.05	85C	0.01	1.31	1.45	103	UNF
2	20	0.05	85C	0.01	1.07	1.26	82	UNF
3	60	0.05	85C	0.01	1.23	1.34	138	CRW
4	60	0.15	H10N	0.01	1.51	1.71	267	CRW
5	40	0.25	86C	0.02	1.42	1.89	371	UNF
6	20	0.15	86C	0.02	1.39	1.57	404	UNF
7	40	0.25	H10N	0.01	1.63	1.91	235	CRW
8	20	0.05	85C	0.02	1.24	1.39	101	UNF
9	40	0.15	85C	0.02	1.37	1.61	369	CRW
10	40	0.15	85C	0.02	1.30	1.41	217	UNF
11	40	0.15	85C	0.02	1.28	1.40	240	UNF
12	20	0.15	H10N	0.02	1.47	1.66	332	UNF
13	40	0.05	86C	0.02	1.16	1.42	337	UNF
14	40	0.05	86C	0.02	1.35	1.52	233	UNF
15	60	0.15	86C	0.02	1.40	1.58	223	UNF
16	60	0.15	86C	0.02	1.38	1.56	247	UNF
17	60	0.25	85C	0.01	1.47	1.72	378	CRW
18	20	0.25	85C	0.01	1.55	1.73	410	CRW
19	20	0.25	85C	0.01	1.54	1.72	370	CRW
20	20	0.15	86C	0.03	1.49	1.48	232	UNF
21	60	0.25	85C	0.02	1.37	1.69	335	UNF
22	20	0.15	H10N	0	1.53	1.79	341	CRW
23	60	0.15	H10N	0	1.48	1.93	328	CRW
24	40	0.25	86C	0	1.48	1.83	362	CRW
25	40	0.15	85C	0.02	1.34	1.67	225	UNF
26	40	0.05	H10N	0.01	1.27	1.58	107	CRW
27	40	0.25	H10N	0.01	1.70	1.75	500	CRW
28	40	0.05	H10N	0.01	1.27	1.61	114	UNF
29	40	0.15	85C	0.01	1.40	1.60	217	CRW
30	40	0.15	85C	0.01	1.45	1.83	240	CRW

*CRW, crown; UNF, uniform.

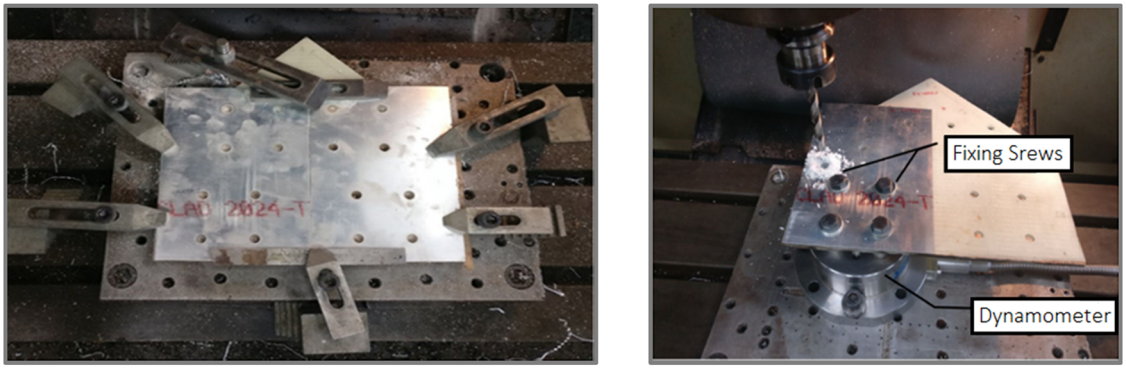

(a) (b)

Figure 1: (a) Drill holes for fixing the hybrid composite plate and (b) experimental setup.

software was used for the analysis of the holes. The treatment of tones, contrast, brightness, and formatting with a binary image filter was performed to evaluate the variables used to calculate the adjusted delamination factor (F_{da}). The segmented image (Figure 2b) was used to determine the delamination area (A_d) and the respective diameter. F_d and F_{da} values were correspondingly calculated according to equations (1) and (2).

The macroscopic analysis of the burrs was performed using a portable digital microscope Dino-Lite Pro model AM-413ZT with 50x amplification used at the hole exit. Then, the types of burrs formed during the drilling process were determined. After assessing the delamination defects associated with the drilled holes, BBD methodology, which is implemented in the Minitab® 19 software, was used to analyze the influence of each input delamination parameter (F_{da_E} and F_{da_S}) and thrust force (F_t), considering a 95% confidence interval (p-value ≤0.05). Besides, an evaluation of the burr type on drilling AA2024 was performed via the comparative visual analysis.

3 Results and discussion

Table 4 presents the control factors and response variables, and Figure 3 depicts the results for the response variables as a function of the control factors for the drilled holes.

The ANOVA of the response variables is presented in Table 5. Besides, for a statistical investigation through the response surface, Figure 4 presents the 3D surface plots according to the analyzed variables.

3.1 Delamination factor

The adjusted delamination factor was calculated by using image processing techniques. In Figure 3, the error bars represent the most relevant measurement variation concerning the average value. This figure shows a comparison between F_{da_E} values generated at the tool entrance

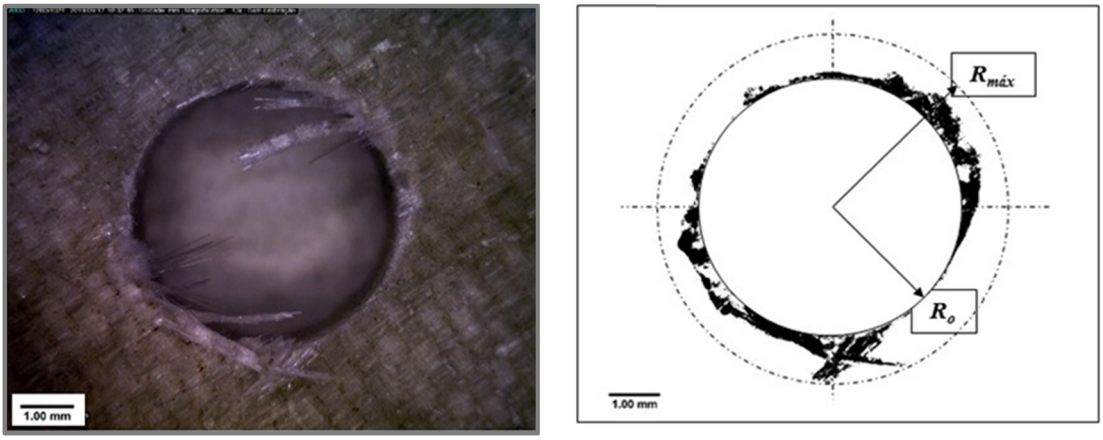

(a) (b)

Figure 2: Output hole 1: (a) original image and (b) segmented image used for the calculation of F_{da}.

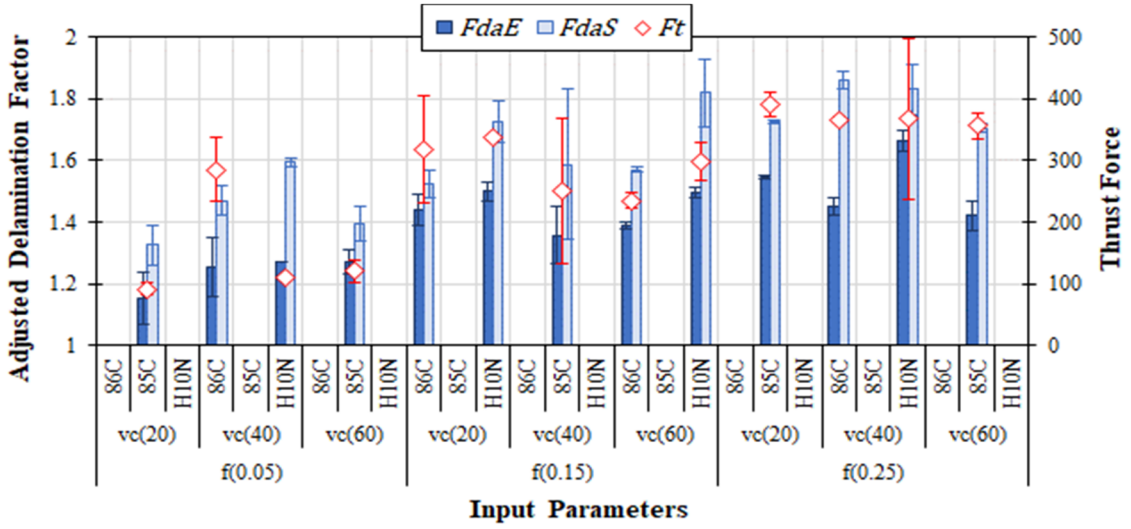

Figure 3: Adjusted delamination factor in the entrance and exit of the GFRP and thrust force.

(peel-up) with F_{da_S} values produced at the tool exit (push-out). It was noted that the second one always shows higher values than the first one [17]. The increase in F_t, F_{da_E}, and F_{da_S} agrees with the increase in the feed rate (f). However, the same behavior is not observed compared to the cutting speed (v_c), which has less influence on the response variables, as presented in Table 5. These results are similar to those obtained by Silva [16] and Malacarne et al. [21], who showed significant differences with different advances and tip angles. Gaitonde et al. [27] observed a similar behavior (reduction of delamination defects with the decrement of feed and cutting speed), but they considered the tip angle as a significant factor. Therefore, it is relevant to consider the effect of geometry on the observed results, as well.

The highest F_{da_E} values were observed when using H10N drill combined with the highest f (0.25 mm rev^{-1}), as presented in Table 5 and highlighted in Figure 4, demonstrating its significance in the experiment. When the highest f value was applied, the highest F_{da_S} and F_t values were also observed. Bold values indicate that the influence of controllable input factors on the output response variables is significant for 95% confidence interval (p-value equal and lower than 0.05).

These results have shown the strong influence of the feed rate on the response variables. It should also be noted that the errors associated with the output variables can be reduced by increasing the number of runs. Table 5 presents that the feed rate (f), the drill type (linear and quadratic effects), and combinations of the feed rate with the cutting speed ($f \times v_c$) and the drill type ($f \times$ drill) have

Table 5: ANOVA of the response variables

Input parameters (controllable factors)	Response variables					
	F_{da_E}		F_{da_S}		F_t	
	p-value	Contr. (%)	p-value	Contr. (%)	p-value	Contr. (%)
f (mm rev^{-1})	<**0.001**	59.04	<**0.001**	49.45	<**0.001**	56.46
v_c (m min^{-1})	0.645	0.15	0.622	0.35	0.395	1.19
Drill	**0.003**	7.41	**0.026**	8.17	0.534	0.63
$f \times f$	0.226	1.68	0.827	0.17	0.632	0.59
$v_c \times v_c$	0.402	0.22	0.364	1.84	0.960	0.01
Drill × drill	**0.002**	9.06	**0.013**	10.41	**0.116**	4.25
$f \times v_c$	**0.011**	5.25	0.989	<0.01	0.551	0.58
$f \times$ drill	**0.033**	3.53	0.358	1.25	**0.104**	4.55
$v_c \times$ drill	0.584	0.21	0.740	0.16	0.672	0.29
R^2	86.2%		71.8%		74.3%	

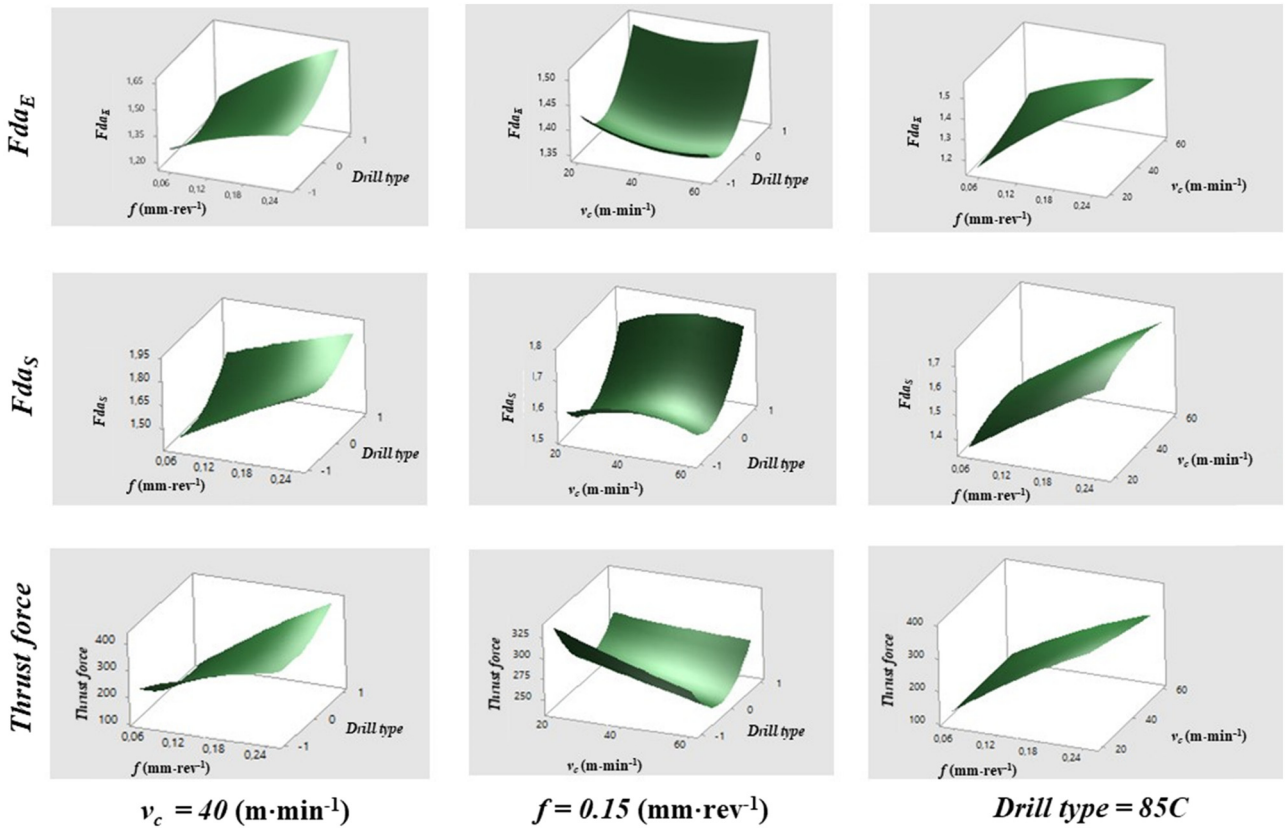

Figure 4: 3D surface plot of response variables.

significant influence (contributions of 59.0, 16.5, 5.25, and 3.53%, respectively) on the adjusted delamination factor at the hole entrance (F_{da_E}) from the peel-up of the GFRP. The R^2 was 86.2%. Through Figure 3 and Figure 4, the adjusted delamination factor at the hole entrance tends to be smaller when $f = 0.05$ mm rev^{-1}. Considering $v_c = 20$ m min^{-1}, drill 85C (0) is the most suitable (run 2), but for $v_c = 40$ m min^{-1}, drill 86C (–1) is the recommended one (run 13). It was confirmed based on the results of F_{da_E} (1.07 and 1.16) presented in Table 4. High friction during drilling (contact between the drill and the hole wall) promotes high temperatures that increase when increasing v_c. Moreover, high temperatures reduce the composite strength, which shows polymer matrix failures, as already observed in the previous studies [21,24,29]. In some cases, as reported by Rubio et al. [32], when high cutting speeds (HSC) were evaluated, there was a highlight for improving the quality of the hole. This condition demonstrates the change in the removed material's geometry because the process conditions promote less pulling of fibers and induce the matrix's softening, facilitating its removal.

Considering the adjusted delamination factor at the tool exit (F_{da_S}) due to the push-out of GFRP (Table 5), the feed rate is also a relevant parameter (49.4%), followed by the drill type with a contribution of 18.6% (linear and quadratic effects). The R^2 was 71.1%. The surface graphs (Figure 4) for the drill 85C (0) (runs 2 and 8) show that F_{da_S} is lower than 1.40, considering $v_c = 20$ m min^{-1} and $f = 0.05$ mm rev^{-1}, which is presented in Table 4. The results show the degree of relevance regarding the drill characteristics, such as the point angle, helix angle, and core thickness. Thus, it is possible to highlight that tool variables can significantly influence the composite's drilling process, as also mentioned by other researchers [16,29,41], showing the relevance of monitoring geometric characteristics. Indeed, these parameters change the cutting characteristics such as shear area, the facility of chip removal, and the tendency to increase the thrust force in the center of the tool.

3.2 Thrust force

Concerning the analysis of the thrust force (F_t) (Table 5), the feed rate was the most significant parameter (56.5%), as mentioned by Zitoune et al. [6]. The drill type (quadratic effect) and its combination with the feed rate ($f \times$ drill) were partially significant (4.25 and 4.55%, respectively). The R^2 was 74.3%. The surface plots (Figure 4) show a

decreasing trend in F_t with decreasing f and increasing v_c for 85C drill type. This fact can be related to the material removed rate (MRR). Moreover, the 85C drill contributes to the lowest F_t values since it has modified geometry on the tool tip, resulting in less damage to the analyzed materials.

The 85C drill, compared to the others, has the smallest point angle (118°), which reduces the contact area of the tool-tip with the material. Likewise, its smallest core thickness (1.45 mm) combined with the smallest chisel edge (0.073 mm) contributes to the centralizing effect, reducing vibrations and resulting in less surface roughness, as shown by Astakhov [41]. Astakhov studied the roughness analysis to provide specifications of the surface quality level associated with the process qualification level. Borba et al. [48] showed that when cross sharpening is used, small chisel edge values (low effect of negative rake angle in the center of the drill) generate low F_t values. The same effect was observed by Gaitonde et al. [27] who showed the contribution of the low feed rate combined with the smallest tip angle, resulting in lower thrust force. This effect is associated with a smaller shear area promoted by the smaller angle.

According to Kumar and Sing [3] and Wang et al. [42], thrust force (F_t) and delamination (F_d) are tightly linked since an increase in the feed rate (f) promotes an increase in F_t, inducing an increase in F_d. Therefore, minimizing F_t reduces F_d. According to Table 4, when run 2 was generated, the lowest values were observed for F_t (82 N), F_{da_E} (1.07), and F_{da_S} (1.26).

3.3 Burrs

The burrs generated at the exit of the AA2024 plate were analyzed macroscopically, and two specific types were identified: crown (CRW) and uniform (UNF) (Figure 5). In the visual analysis, the uniform burr with drill cap (UDC) was considered a variation of the uniform burr (UNF) because they are caused by the same mechanism [43]. The hat type was not observed. As they are easier to remove, uniform burrs are preferable [33]. The UNF conditions and the absence of significant burrs were observed in 53.3% of the total holes (i.e., 1, 2, 5, 6, 8, 10, 11, 12, 13, 14, 15, 16, 20, 21, 25, and 28). In other holes, there was an undesirable CRW (46.7% of the total). The trend of better results occurred using the 86C drill with $v_c \leq 40\ \mathrm{m\ min^{-1}}$ and $f \leq 0.15\ \mathrm{mm\ rev^{-1}}$. According to Pinto [34], smaller feed rate (f) values generate lower thrust force (F_t), and a higher point angle (σ) tends to produce a distributed circular load of the holes, promoting total or partial burr fracture. This scenario can be associated with the 86C drill, which has these geometric features.

For some sets of holes (i.e., 1, 3, 5, 12, 17, 21, 22, 24, 26, and 28), differences were observed between the burr types despite having the same cutting parameters. These demonstrate the need for additional characterization of analyzes, such as checking the burr height, microstructural analysis, and hardness analysis to quantify and classify differences in their formation. According to Ko and Lee [33] and Pinto [34], in some situations, the cutting parameters can be near to promote the transition point among the type of burr – crown and uniform – staying within the margin of error of the results. For some instances, these differences may be associated with other factors, such as holes 1 and 3, which presented close thrust force values (F_t) equal to 103 and 138 N, respectively. These results may be related to the vicinity of the fracture point for this condition. Therefore, as pointed by Dornfeld et al. [44] and Manjunatha [45], even for the same type of burrs (whether UNF or CRW), burr's height, slope, shape, and mechanical characteristics need further analysis.

The holes 9, 29, and 30 resulted in similar F_{da_E} and F_{da_S} values and presented the same burr type (CRW).

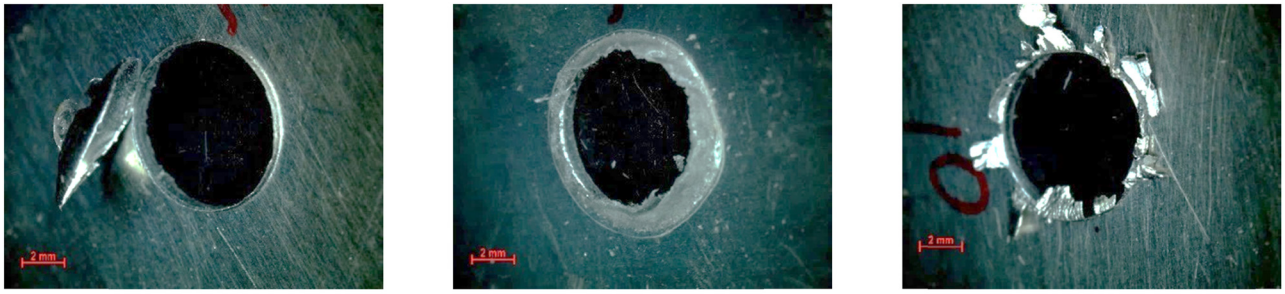

Figure 5: Burr types: (a) uniform (with drill cap), (b) uniform, and (c) crown.

These characteristics can be attributed to the 85C tool geometry and, mostly, to the point angle (118°), as observed by Srinivasan et al. [25] and Durão et al. [46] who associated the burr with the geometric features of the tool. However, run 9 presented higher thrust force (369 N) in comparison to runs 29 and 30 (217 N and 240 N, respectively). Therefore, the only modification observed was the run-out (δ) of the drill 85C (run 9, $\delta = 0.02$ mm; runs 29 and 30, $\delta = 0.01$ mm), which may have caused an increase in F_t value due to the increase of vibrations in the cutting process. According to Tsao and Hocheng [47], the vibration can even interfere in the burrs formation, and it can be related to run-out deviations. Those deviations can generate differences in roughness, but it was not investigated in the present study.

Although holes 10, 11, and 25 had been made using the same cutting conditions as holes 9, 29, and 30, and obtained similar F_t values, the burr shapes were different. In other words, UNF was observed in the first one and CRW was observed in the second one, which is usually associated with the drill point angle and its sharpening [33,43]. However, the same drill type was used (85C), and any kind of failure (tool wear or tool fracture) was not detected. Thus, complementary analyses are necessary to identify and associate the burr parameters (hardness and height) because these can be set in the transition zone between the burr types.

3.4 Parameter optimization

The multivariate optimization of control variables was performed through BBD based on the response variables to minimize the delamination (tool entrance and tool exit) and thrust force simultaneously. Thus, optimized parameters were obtained such as drilling with the 85C drill applying $v_c = 20\ \text{m min}^{-1}$ and $f = 0.05\ \text{mm rev}^{-1}$, which will give the following estimated responses: $F_{da_E} = 1.15$, $F_{da_S} = 1.36$, and $F_t = 90.6$ N.

Table 6: Estimated and experimented response variables

	F_{da_E}	F_{da_S}	F_t (N)
Estimated	1.15	1.36	90.6
Experimented	1.18	1.33	67.3
Error (%)	2.54%	2.25%	25.7%

Drilling conditions: $v_c = 20\ \text{m min}^{-1}$, $f = 0.05\ \text{mm rev}^{-1}$, and drill 85C.

A validation test was performed using the optimized parameters obtained via BBD. Then, three holes were drilled and evaluated to check if those parameters reach the estimated responses mentioned earlier. Table 6 presents the average of the experimental results. The experimental values of F_{da_E} and F_{da_S} were similar to those predicted values (with an error lower than 3%). The peel-up and push-out phenomena were small in the fibers and polymer matrix. Conversely, the experimental thrust force was about 25.7% lower than the estimated F_t. The low parameters used (v_c, f) and drill point angle 85C ($\sigma = 118°$) were relevant for good results. Similar results and observations were highlighted previously by Srinivasan et al. [25].

Although the burr type was not analyzed via BBD, the optimized condition promoted a CRW type, which is not recommended for the drilling process due to the need for rework to remove this element. Figure 6 shows the images of the burrs obtained in the validation test.

As commented in the literature [35,36], the UNF burrs, with less complicated removal, are associated with a distributed circular load of the holes, unlike CRW burrs, more irregular and laborious removal. The CRW type, predominant in optimization tests, is related to smaller point angles, as shown in the 85C drill (118°), and the consequent deformation in the hole center region. Silva et al. [37] recommend avoiding the deburring step

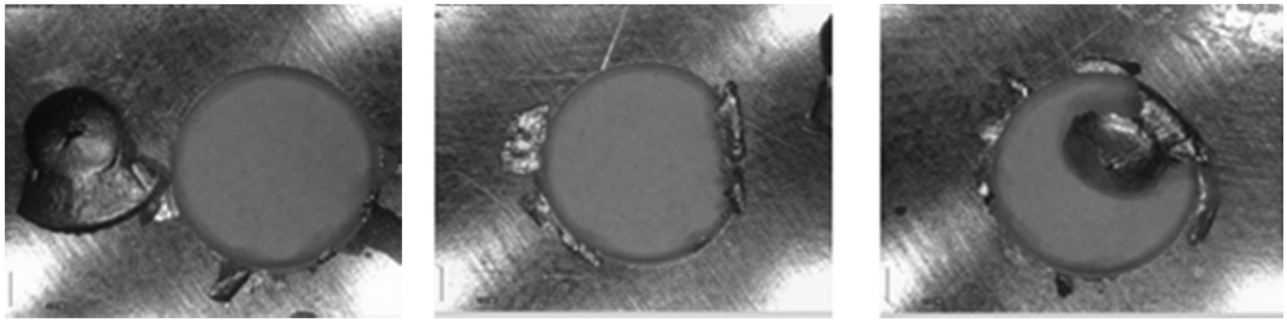

Figure 6: Burr holes after drilling with optimized parameters.

because this rework leads to additional manufacturing costs, making the process unfeasible. The generation of uniform burrs with short height should be the priority goal. In most cases, this rework is carried out manually without adding value to the product.

4 Conclusion

It was evaluated the influence of cutting conditions over the delamination factor and thrust force of metal-composite laminate. The present work investigated a sandwich plate composite by AA2024/GFRP/AA2024 joint. According to the results for this specific case study, it is possible to have some relevant conclusions and, mainly, recommendations for drilling metal-composite laminates used in aeronautical joints:

- The thrust force (F_t) during drilling depends significantly on the feed rate (f). Another partially significant factor is the drill type (combined or not with f).
- f and drill are control variables that influence the adjusted delamination factor significantly at the input (F_{da_E}) and output (F_{da_S}) of the GFRP.
- The cutting speed (v_c) does not affect significantly F_t and F_{da_S}. However, the combination $f \times v_c$ is significant in F_{da_E}.
- The optimization of the cutting parameters via BBD can obtain values close to those estimated for the response variables (F_{da_E}, F_{da_S}, and F_t). The optimized levels were $v_c = 20$ m min^{-1}, $f = 0.05$ mm rev^{-1}, and drill type 85C for the investigated metal-composite laminate.
- In case of the burrs at the hole output of AA2024 using the optimized parameters, the results are unsatisfactory (crown type), which requires further investigations on the optimal hybrid stack drilling.

Acknowledgments: The authors thank TAP Air Portugal Co. for the donation of the AA 2024 sheets, Sandvik Coromant Co. for the donation of the uncoated drill tools, CAPES (grant 88882.346387/2019-01), and CNPq (process 310656/2018-4 and 134587/2018-9) for financial support.

Conflict of interest: Authors state no conflict of interest.

References

[1] Liu DF, Tang YJ, Cong WL. A review of mechanical drilling for composite laminates. Comp Struct. 2012;94(4):1265–79. doi: 10.1016/j.compstruct.2011.11.024.

[2] Bhagwat PM, Ramachandran M, Raichurkar P. Mechanical properties of hybrid glass/carbon fiber reinforced epoxy composites. Mater Today: Proc. 2017;4(8):7375–80. doi: 10.1016/j.matpr.2017.07.067.

[3] Kumar D, Sing KK. Experimental analysis of delamination, thrust force and surface roughness on drilling of glass fibre reinforced polymer composites material using different drills. Mater Today: Proc. 2017;4(8):7618–27. doi: 10.1016/j.matpr.2017.07.095.

[4] Xu J, El Mansori M. Experimental study on drilling mechanisms and strategies of hybrid CFRP/Ti stacks. Comp Struct. 2016;157:461–82. doi: 10.1016/j.compstruct.2016.07.025.

[5] Akhil KT, Shunmugesh K, Aravind S, Pramodkumar M. Optimization of drilling characteristics using grey relational analysis (GRA) in glass fiber reinforced polymer (GFRP). Mater Today: Proc. 2017;4(2, Part A):1812–9. doi: 10.1016/j.matpr.2017.02.024.

[6] Zitoune R, Krishnaraj V, Collombet F. Study of drilling of composite material and aluminium stack. Comp Struct. 2010;92(5):1246–55. doi: 10.1016/j.compstruct.2009.10.010.

[7] Ning H, Li Y, Hu N, Arai M, Takizawa N, Liu Y, et al. Experimental and numerical study on the improvement of interlaminar mechanical properties of Al/CFRP laminates. J Mater Process Technol. 2015;216:79–88. doi: 10.1016/j.jmatprotec.2014.08.031.

[8] Khashaba UA, El-Keran AA. Drilling analysis of thin woven glass-fiber reinforced epoxy composites. J Mater Process Technol. 2017;249:415–25. doi: 10.1016/j.jmatprotec.2017.06.011.

[9] Lazar M-B, Xirouchakis P. Experimental analysis of drilling fiber reinforced composites. Int J Mach Tools Manufacture. 2011;51(12):937–46. doi: 10.1016/j.ijmachtools.2011.08.009.

[10] Krishnaraj V, Zitoune R, Collombet F. Comprehensive review on drilling of multimaterial stacks. J Mach Form Technol. 2010;2(3–4):171–200. https://www.researchgate.net/publication/273127359

[11] Kihlman H, Ossbahr G, Engström M, Anderson J. Low-cost automation for aircraft assembly. Proceedings of the SAE Aerospace Manufacturing & Automated Fastening Conference & Exhibition. St. Louis, MS, USA: SAE International; 2004 Sept. 20–23. p. 8. doi: 10.4271/2004-01-2830.

[12] Palanikumar K. Experimental investigation and optimisation in drilling of GFRP composites. Measurement. 2011;44(10):2138–48. doi: 10.1016/j.measurement.2011.07.023.

[13] Zitoune R, Krishnaraj V, Collombet F, Le Roux S. Experimental and numerical analysis on drilling of carbon fibre reinforced plastic and aluminium stacks. Comp Struct. 2016;146:148–58. doi: 10.1016/j.compstruct.2016.02.084.

[14] Davim JP, editor. Machining composites materials. London: John Wiley & Sons; 2013.

[15] Kumar D, Singh K. Investigation of delamination and surface quality of machined holes in drilling of multiwalled carbon nanotube doped epoxy/carbon fiber reinforced polymer nanocomposite. Proc Inst Mech Eng, Part L: J Mater: Des Appl. 2017;233(4):647–63. doi: 10.1177/1464420717692369.

[16] Silva JA. Analysis of drilling glass-fiber reinforced polyester composite Thesis (M.Sc.) in Mechanical Engineering. Florianópolis. SC, Brazil: POSMEC-UFSC; 2015. p. 117.

(in Portuguese). https://repositorio.ufsc.br/xmlui/handle/123456789/160729
[17] Ho-Cheng H, Dharan CKH. Delamination during drilling in composite laminates. J Eng Ind (Trans ASME). 1990;112(3):236–9. doi: 10.1115/1.2899580.
[18] Davim JP, Rubio JC, Abrão AM. A novel approach based on digital image analysis to evaluate the delamination factor after drilling composite laminates. Compos Sci Technol. 2007;67(9):1939–45. doi: 10.1016/j.compscitech.2006.10.009.
[19] Velaga M, Cadambi RM. Drilling of GFRP composites for minimising delamination effect. Mater Today: Proc. 2017;4(10):11229–36. doi: 10.1016/j.matpr.2017.09.044.
[20] Rakesh PK, Singh I, Kumar D. Flexural behaviour of glass fibre-reinforced plastic laminates with drilled hole. Proc Inst Mech Eng, Part L: J Mater: Des Appl. 2012;226(2):149–58. doi: 10.1177/1464420711430007.
[21] Malacarne DK, Devitte C, Souza AJ. Drilling parameters optimization for quality holes in GFRP via Box-Behnken Design. Annals of the 10th Brazilian Congress of Manufacturing Engineering. São Carlos, SP, Brazil: ABCM; 2019 Aug. 5–7. p. 5. (in Portuguese). https://www.researchgate.net/publication/335507306
[22] Durão LMP, Gonçalves DJS, Albuquerque VHC, Tavares JMRS. Evaluation of tools for drilling laminates. Annals of the 8th National Congress of Experimental Mechanics. Guimarães, Portugal: APAET; 2010 April 21–23. p. 10. (in Portuguese). https://www.researchgate.net/publication/261834447
[23] Feito N, Álvarez JD, Álvarez AD, Cantero JL, Miguélez MH. Experimental analysis of the influence of drill point angle and wear on the drilling of woven CFRPs. Mater (Basel). 2014;7(6):4258–71. doi: 10.3390/ma7064258.
[24] Karimi NZ, Heidary H, Ahmadi M. Residual tensile strength monitoring of drilled composite materials by acoustic emission. Mater Des. 2012;40:229–36. doi: 10.1016/j.matdes.2012.03.040.
[25] Srinivasan T, Palanikumar K, Rajagopal K, Latha B. Optimization of delamination factor in drilling GFR-polypropylene composites. Mater Manuf Process. 2017;32(2):226–33. doi: 10.1080/10426914.2016.1151038.
[26] Batista MF, Rodrigues AR, Basso IF, Toti FA, Oliveira FB. Method for assessing hole damages in composites materials. Annals of the 9th Brazilian Congress of Manufacturing Engineering. Joinville, SC, Brazil: ABCM; 2017 July 26–29. p. 9. https://www.researchgate.net/publication/319995629
[27] Gaitonde V, Karnik SR, Rubio JC, Correia AE, Abrao AM, Davim JP. Analysis of parametric influence on delamination in high-speed drilling of carbon fiber reinforced plastic composites. J Mater Process Technol. 2008;203(1–3):431–8. doi: 10.1016/j.jmatprotec.2007.10.050.
[28] Davim JP, Reis P, Antonio CC. Experimental study of drilling glass fiber reinforced plastics (GFRP) manufactured by hand lay-up. Compos Sci Technol. 2004;64(2):289–97. doi: 10.1016/S0266-3538(03)00253-7.
[29] Rubio JC, Silva LR, Abrão AM, Faria PE, Correia AE, Davim JP. Furação com alta velocidade de corte em compósitos poliméricos reforçados com fibras de vidro. Ciência Tecnol dos Materiais. 2007;19(3–4):83–7. http://www.scielo.mec.pt/pdf/ctm/v19n3-4/19n3-4a10.pdf
[30] Davim JP, Reis P. Study of delamination in drilling carbon fiber reinforced plastics (CFRP) using design experiments. Comp Struct. 2003;59(4):481–7. doi: 10.1016/S0263-8223(02)00257-X.
[31] Abrão AM, Rubio JC, Faria PE, Davim JP. The effect of cutting tool geometry on thrust force and delamination when drilling glass fibre reinforced plastic composite. Mater Des. 2008;29(2):508–13. doi: 10.1016/j.matdes.2007.01.016.
[32] Rubio JC, Abrao AM, Faria PE, Correia AE, Davim JP. Effects of high speed in the drilling of glass fibre reinforced plastic: evaluation of the delamination factor. Int J Mach Tools Manuf. 2008;48(6):715–20. doi: 10.1016/j.ijmachtools.2007.10.015.
[33] Ko S-L, Lee J-K. Analysis on burr formation in drilling with new concept drill. J Mater Process Technol. 2001;113(1–3):392–8. doi: 10.1016/S0924-0136(01)00717-8.
[34] Pinto GTB. Influence Spec drill geometry Drill aeronautical thin-sheets Thesis (M.Sc.) in Mechanical Engineering. Florianópolis. SC, Brazil: POSMEC-UFSC; 2010; p. 164. (in Portuguese). http://repositorio.ufsc.br/xmlui/handle/123456789/93674
[35] Ko S-L, Chang J-E, Yang G-E. Burr minimizing scheme in drilling. J Mater Process Technol. 2003;140(1–3):237–42. doi: 10.1016/S0924-0136(03)00719-2.
[36] Ballou JR, Joshi SS, DeVor RE, Kapoor SG. Burr formation in drilling intersecting holes with machinable austempered ductile iron (MADI™). J Manuf Process. 2007;9(1):35–46. doi: 10.1016/S1526-6125(07)70106-8.
[37] Silva JD, Saramago SFP, Machado AR. Optimization of the cutting conditions (Vc, fz e doc) for burr minimization in face milling of mould steel. J Brazillian Soc Mech Sci Eng. 2009;31(2):151–60. doi: 10.1590/S1678-58782009000200008.
[38] Paiva JMF, Mayer S, Cândido G, Rezende MC. Evaluation of glass transition temperature of the repaired polymeric composites of aeronautical use. Polímeros. 2006;16(1):79–87. (in Portuguese). doi: 10.1590/S0104-14282006000100016.
[39] Garcia RF, Feix EC, Mendel HT, Gonzalez AR, Souza AJ. optimization of cutting parameters for finish turning of 6082-T6 aluminum alloy under dry and RQL conditions. J Braz Soc Mech Sci Eng. 2019;41(A):317. doi: 10.1007/s40430-019-1826-4.
[40] Ferreira SLC, Bruns RE, Silva EGP, Santos WNL, Quintella CM, David JM, et al. Statistical designs and response surface techniques for the optimization of chromatographic systems. J Chromatogr A. 2007;1158(1–2):2–14. doi: 10.1016/j.chroma.2007.03.051.
[41] Astakhov VP. Geometry of single-point turning tools and drills: fundamentals and practical applications. London: Springer-Verlag; 2010. doi: 10.1007/978-1-84996-053-3.
[42] Wang C-Y, Chen Y-H, An Q-L, Cai X-J, Ming W-W, Chen M. Drilling temperature and hole quality in drilling of CFRP/aluminum stacks using diamond coated drill. Int J Precis Eng Manuf. 2015;16(8):1689–97. doi: 10.1007/s12541-015-0222-y.
[43] Aurich JC, Dornfeld D, Arrazola PJ, Franke V, Leitz L, Min S. Burrs – analysis, control and removal. CIRP Ann. 2009;58(2):519–42. doi: 10.1016/j.cirp.2009.09.004.
[44] Dornfeld DA, Kim JS, Dechow H, Hewson J, Chen LJ. Drilling burr formation in titanium alloy Ti-6Al-4V. CIRP Ann. 1999;48(1):73–6. doi: 10.1016/S0007-8506(07)63134-5.
[45] Manjunatha NN. ANN Model Predict Burr Height Thickness Thesis (M.Sc.). Kansas, USA: Department of Industrial and Manufacturing Engineering, Graduate School of Wichita State University; 2007; p. 101. http://hdl.handle.net/10057/1147

[46] Durão LMP, Gonçalves DJS, Tavares JMRS, Albuquerque VHC, Marques AT. Comparative analysis of drills for composite laminates. J Comp Mater. 2012;46(14):1649–59. doi: 10.1177/0021998311421690.
[47] Tsao CC, Hocheng H. The effect of chisel length and associated pilot hole on delamination when drilling composite materials. Int J Mach Tools Manuf. 2003;43(11):1087–92. doi: 10.1016/S0890-6955(03)00127-5.
[48] Borba RB, Ribeiro Filho SLM, Brandão LC. Influence of different types of sharpening in straight flute drills on burr formation. Acta Sci Technol. 2016;38(4):465–8. doi: 10.4025/actascitechnol.v38i4.29222.